Neuroscience 326 (2016) 126–140

INHIBITORY CONTROL OF ASCENDING GLUTAMATERGIC PROJECTIONS TO THE LAMPREY RESPIRATORY RHYTHM GENERATOR

ELENIA CINELLI, DONATELLA MUTOLO, MASSIMO CONTINI, TITO PANTALEO AND FULVIA BONGIANNI *

Dipartimento di Medicina Sperimentale e Clinica, Sezione Scienze Fisiologiche, Università degli Studi di Firenze, Viale G.B. Morgagni 63, 50134 Firenze, Italy

Abstract—Neurons within the vagal motoneuron region of the lamprey have been shown to modulate respiratory activity via ascending excitatory projections to the paratrigeminal respiratory group (pTRG), the proposed respiratory rhythm generator. The present study was performed on *in vitro* brainstem preparations of the lamprey to provide a characterization of ascending projections within the whole respiratory motoneuron column with regard to the distribution of neurons projecting to the pTRG and related neurochemical markers. Injections of Neurobiotin were performed into the pTRG and the presence of glutamate, GABA and glycine immunoreactivity was investigated by double-labeling experiments. Interestingly, retrogradely labeled neurons were found not only in the vagal region, but also in the facial and glossopharyngeal motoneuron regions. They were also present within the sensory octavolateral area (OLA). The results show for the first time that neurons projecting to the pTRG are immunoreactive for glutamate, surrounded by GABA-immunoreactive structures and associated with the presence of glycinergic cells. Consistently, $GABA_A$ or glycine receptor blockade within the investigated regions increased the respiratory frequency. Furthermore, microinjections of agonists and antagonists of ionotropic glutamate receptors and of the $GABA_A$ receptor agonist muscimol showed that OLA neurons do not contribute to respiratory rhythm generation. The results provide evidence that glutamatergic ascending pathways to the pTRG are subject to a potent inhibitory control and suggest that disinhibition is one important mechanism subserving their function. The general characteristics of inhibitory control involved in rhythmic activities, such as respiration, appear to be highly conserved throughout vertebrate evolution.

Key words: control of breathing, inhibitory amino acids, glutamatergic transmission.

INTRODUCTION

The isolated brainstem of the adult lamprey, a lower vertebrate that diverged from the main vertebrate line ~560 million years ago (Kumar and Hedges, 1998), spontaneously generates a stable and regular respiratory neuronal activity *in vitro* (fictive respiration) for at least 12 h; this activity is very similar to that underlying respiration in intact animals (Rovainen, 1977, 1983; Thompson, 1985; Russell, 1986; Bongianni et al., 1999, 2002, 2006; Mutolo et al., 2007, 2010, 2011;Martel et al., 2007; Cinelli et al., 2013, 2014). The lateral walls of its central nervous system consist of two longitudinal zones or plates: the ventral primarily motor basal plate and the dorsal primarily sensory alar plate that comprises the octavolateral area (OLA; see e.g. Nieuwenhuys, 1972; Villar-Cerviño et al., 2008). Respiratory motoneurons are located in the facial, glossopharyngeal and, especially, in the vagal nuclei (Rovainen, 1974, 1977, 1979; Guimond et al., 2003), while the putative central neural mechanisms generating the respiratory rhythmic activity are located in the paratrigeminal respiratory group (pTRG), rostral to the trigeminal motor nucleus (Mutolo et al., 2007, 2010, 2011; Cinelli et al., 2013, 2014; Bongianni et al., 2016).

Endogenously released excitatory amino acids, but not GABA and glycine, have been shown to have an essential role in the respiratory rhythmogenesis (Rovainen, 1983; Martel et al., 2007; Bongianni et al., 1999, 2006, 2016; Cinelli et al., 2013, 2014). Only GABAergic influences have a modulatory role at the pTRG level. On the other hand, GABAergic and glycinergic inputs to neurons within the vagal motoneuron region mediate changes in respiratory frequency through ascending excitatory projections to the pTRG (Cinelli et al., 2014). However, an extensive characterization of the facial, glossopharyngeal and vagal motoneuron regions is still lacking with regard to projections to the pTRG and related neurochemical markers such as glutamate, GABA and glycine.

*Corresponding author. Tel: +39-055-2751608; fax: +39-055-4379506.
E-mail address: fulvia.bongianni@unifi.it (F. Bongianni).

Abbreviations: I_1, isthmic Müller cell; MRRN, middle rhombencephalic reticular nucleus; NOMI, intermediate octavomotor nucleus; NOMP, posterior octavomotor nucleus; NTS, nucleus tractus solitarii; nVm, motor root of the trigeminal nerve; nVs, sensory root of the trigeminal nerve; nVIII, vestibular nerve; nIX, glossopharyngeal nerve; nX, vagal nerve; OLA, octavolateral area; PB, phosphate buffer; PBS, phosphate-buffered saline; PRRN, posterior rhombencephalic reticular nucleus; pTRG, paratrigeminal respiratory group; rdV, descending root of the trigeminal nerve; SL, sulcus limitans of His; VA, raw vagal nerve activity; V, trigeminal motor nucleus; VII, facial motor nucleus; IX, glossopharyngeal motor nucleus; X, vagal motor nucleus.

http://dx.doi.org/10.1016/j.neuroscience.2016.03.063
0306-4522/

The present study was performed on *in vitro* brainstem preparations of the lamprey to investigate whether retrogradely labeled neurons could be identified within the whole respiratory motoneuron column by injections of Neurobiotin into the pTRG. The presence of glutamate, GABA and glycine immunoreactivity within the projection areas was ascertained by double-labeling experiments and the responses to microinjections of bicuculline or strychnine into the same regions were investigated.

In addition, since retrogradely labeled neurons were found in the alar plate within the OLA, the distribution of glutamate, GABA and glycine immunoreactivity was investigated and microinjections of bicuculline and strychnine were also performed in this region. An attempt was made to disclose a possible role of this portion of the OLA in respiratory rhythm generation by using microinjections of ionotropic glutamate receptor agonists and antagonists as well as of the $GABA_A$ receptor agonist muscimol.

EXPERIMENTAL PROCEDURES

Ethical approval

A total of 56 young adult (12–15 cm) lampreys (*Petromyzon marinus*) were employed. All animal care and experimental procedures were conducted in accordance with the Italian legislation and the official regulations of the European Communities Council on the use of laboratory animals (directive 86/609/EEC and 2010/63/UE). The study was approved by the Animal Care and Use Committee of the University of Florence. All efforts were made to minimize animal suffering and to reduce the number of animals used.

Anatomical experiments

Six lampreys were used. For details on animal preparation see Cinelli et al. (2013, 2014). The animals were anaesthetized with tricaine methanesulphonate (100 mg/l; MS 222, Sigma–Aldrich, St Louis, MO, USA) and transected below the gills. The isolated brain-spinal cord was mounted dorsal side up in a Sylgard-lined recording chamber perfused with a cold physiological solution. The chamber volume was 3.0 ml, and the perfusion rate was set at 2.5 ml/min. Bath temperature was set at 9–10 °C. The solution flowed from a reservoir and had the following composition (in mM): 91 NaCl, 2.1 KCl, 2.6 $CaCl_2$, 1.8 $MgCl_2$, 4 glucose, 23 $NaHCO_3$. The solution was bubbled with 95% O_2–5% CO_2 to oxygenate and maintain the pH in the bath at 7.4. The brain was exposed dorsally and a transection was made caudal to the obex. The roof of the isthmic region was cut along the midline and the alar plates were spread laterally and pinned down (see Mutolo et al., 2007, 2010, 2011; Cinelli et al., 2013, 2014).

Retrograde tracing. Unilateral microinjections (~10 nl) of Neurobiotin (20% in distilled water; Vector Laboratories, Burlingame, CA, USA) were performed by means of glass micropipettes (tip diameter 10–20 μm) and by applying pressure pulses with a Picospritzer (General Valve Corporation, Fairfield, NJ, USA) connected to the injection pipette. The inactive dye Fast Green (0.2%, Sigma–Aldrich) was added to the solution to aid visualization of the injected tracer and to verify that the injection was reasonably confined to the investigated region. The localization of the pTRG was judged by the position of the dye spot with respect to the sulcus limitans of His (SL) and the isthmic Müller cell (I_1) (Cinelli et al., 2013, 2014). The depth of the injection (~0.3 mm below the dorsal surface) was inferred from that of rhythmic extracellular neuronal activity previously recorded in each preparation (see below for further details).

Dissection and histology. After Neurobiotin injections, the brains from the six lampreys were kept continuously perfused with the physiological solution in the dark at 4 °C. To allow the retrograde transport of the tracer, a 24-h perfusion period was scheduled. Thereafter, the brains were dissected out of the surrounding tissue and used for the immunohistochemistry (double-labeling experiments). For glutamate immunohistochemistry, two brains were fixed by immersion in 4% formalin, 1% glutaraldehyde and 14% of a saturated solution of picric acid in 0.1 M phosphate buffer (PB). For GABA immunohistochemistry, two brains were fixed by immersion in 4% formalin, 0.25% glutaraldehyde and 14% of a saturated solution of picric acid in PB. For glycine immunohistochemistry, two brains were fixed by immersion in 2% formalin in PB pH 7.4 for 12–24 h. The brains were postfixed for 24–48 h, after which they were cryoprotected in 20% sucrose in PB for 3–12 h. Transverse 20-μm-thick sections were made using a cryostat, collected on gelatin-coated slides and stored at −20 °C until additional processing.

Immunohistochemistry. All primary and secondary antibodies were diluted in 1% BSA, 0.3% Triton-X 100 in 0.1 M PB. For immunohistochemical detection of glutamatergic neurons (double-labeling experiments), sections were incubated overnight with a polyclonal rabbit anti-glutamate antibody (1:600; AB133; Millipore Corporation, Billerica, MA, USA). Following a thorough rinse in 0.01 M phosphate-buffered saline (PBS) the sections were incubated with Alexa Fluor 488 goat anti-rabbit IgG (1:250; Invitrogen, Life Technologies, Carlsbad, CA, USA) and Alexa fluor-568 conjugated streptavidin (1:1000; Invitrogen) for 3 h, rinsed in PBS and coverslipped with glycerol containing 2.5% diazabicyclanooctane (Sigma Aldrich). For the immunohistochemical detection of GABA (double-labeling experiments), sections were incubated overnight with rabbit polyclonal anti-GABA conjugated to BSA with gluteraldehyde (1:1000; NBP1-78346; Novus Biologicals, Cambridge, UK). Sections were subsequently incubated with a mixture of Alexa Fluor 488 goat anti-rabbit IgG (1:200; Invitrogen) and Alexa fluor-568 conjugated streptavidin (1:1000; Invitrogen) for 3 h. For the immunohistochemical detection of glycine (double-labeling experiments), sections were incubated

with rat polyclonal anti-glycine (1.5000; IG1002; ImmunoSolutions, Jesmond, New South Wales, Australia). Sections were subsequently incubated with a mixture of Alexa Fluor 488 goat anti-rat IgG (1:200; Invitrogen) and Alexa fluor-568 conjugated streptavidin (1:1000; Invitrogen) for 3 h. The specificity of the employed glutamate and glycine antibodies is known from previous studies in the lamprey (Mahmood et al., 2009; Stephenson-Jones et al., 2011; Cinelli et al., 2013). Although the rabbit anti-GABA antibody has not been previously used in the lamprey, we are confident that it is specific for GABA. In fact, the pattern of distribution of labeled cells that this antibody produces is similar to that obtained with different anti-GABA antibodies (Robertson et al., 2007; Villar-Cerviño et al., 2008; Cinelli et al., 2014).

Analysis. Retrogradely labeled neurons of the six preparations were counted on transverse sections of the region extending from the facial motor nucleus to the vagal motor nucleus. Every second section was counted to prevent double-counting of single cells, although this procedure could underestimate the total number of counted neurons. Photomicrographs of key results were taken using a Nikon DS-Fi1 (Nikon, Japan) digital camera and software. Illustrations were prepared in Adobe Photoshop CS3 (Adobe Systems Incorporated, San Jose, CA, USA). Images were only adjusted for brightness and contrast. Drawings of serial transverse sections were designed and assembled using Illustrator CS6 software (Adobe Systems Incorporated). The localization of labeled cells was reported on schematic drawings of individual transverse sections. The nomenclature used for anatomical structures is the same as in previous studies (Robertson et al., 2007; Villar-Cerviño et al., 2008; 2013; Cinelli et al., 2013, 2014). The number of neurons in the ipsi- and contralateral side of each investigated area was compared using unpaired t-tests (GraphPad Prism 5, La Jolla, CA, USA). A 40X objective was used to measure the largest diameter of retrogradely labeled cells in one representative preparation (see Results). All values are presented as mean ± SEM. $P < 0.05$ was considered as significant.

Electrophysiological experiments

Experiments were performed on 50 lampreys. Animal preparation and experimental procedures have been already fully described (Bongianni et al., 1999, 2002, 2006; Mutolo et al., 2007, 2010, 2011; Cinelli et al., 2013, 2014). Of note, the preparation was similar to that employed in the anatomical experiments, except that the brain tissue rostral to the optic tectum was cut and removed.

Recording procedures. Suction electrodes were used to record efferent respiratory activity from both vagal nerves. The signals were amplified, full-wave rectified and integrated (low-pass filter, time constant 10 ms). Extracellular neuronal activity was recorded with fine (0.1 mm shaft diameter) tungsten microelectrodes (5 MΩ impedance at 1 kHz). The obex was used to evaluate coordinates of recording and microinjection sites. Neuronal activity was recorded from vagal or glossopharyngeal motoneurons on the basis of anatomical landmarks easily visible under microscope control (0.4–0.6 or 0.6–0.8 mm rostral to the obex, 0.3–0.4 mm lateral to the midline and 0.15–0.25 mm below the dorsal surface) as well as from respiration-related neurons of the pTRG (1.8–2.0 mm rostral to the obex, 0.8–1.0 mm lateral to the midline and 0.25–0.3 mm below the dorsal surface (given the arrangement of our preparations the dorsal surface corresponded to the surface of the tilted lateral wall of the IV ventricle). Raw and integrated signals were acquired and analyzed by a personal computer equipped with an analog-to-digital interface (50 kHz sampling rate; Digidata 1440, Molecular Devices, Sunnyvale, CA, USA), and appropriate software (Axoscope, Molecular Devices) was used. Offline analysis was performed using Clampfit software (Molecular Devices).

Drug application. Drugs were microinjected (0.5–1 nl) into the region of respiratory motoneurons on the basis of extracellular recordings and related coordinates as well as into the OLA at the same levels. Microinjections into the OLA were performed in the proximity of the periventricular area, at about 0.1–0.2 mm below the dorsal surface, i.e. at the depth inferred from the location of retrogradely labeled neurons (see Results). The following drugs were used: 1 mM bicuculline methiodide (a $GABA_A$ receptor antagonist, Sigma–Aldrich), 1 mM strychnine hydrochloride (a glycine receptor antagonist, Tocris Bioscience, Bristol, UK), 2 mM *N*-methyl-D-aspartic acid (NMDA; a selective NMDA receptor agonist, Tocris Bioscience), 1 mM (*S*)-α-amino-3-hydroxy-5-methyl-4-isoxazolepropionic acid (AMPA; a selective non-NMDA receptor agonist, Tocris Bioscience), 5 mM D-(−)-2-amino-5-phosphonopentanoic acid (D-AP5; a NMDA receptor antagonist, Tocris Bioscience), 1 mM 6-cyano-7-nitroquinoxaline-2,3-dione (CNQX; a non-NMDA receptor antagonist, Tocris Bioscience), 0.2 mM muscimol (a $GABA_A$ receptor agonist, Tocris Bioscience). Drug concentrations were similar to those employed in previous studies in lampreys (Cinelli et al., 2013, 2014). All employed drugs were dissolved in distilled water made up to a stock solution and stored as small aliquots in a freezer until use. Stock solutions were diluted in the perfusing solution to the final desired concentration immediately prior to microinjections. Only one drug was tested in each preparation.

Details on microinjection techniques have been provided in our previous reports. The inactive dye Fast Green (0.2%, Sigma–Aldrich) was added to the drug solution to visually assess the spread and the approximate localization of the injection. In six preparations green fluorescent latex microspheres (LumaFluor, New City, NY, USA) were added (dilution 1:3) to the injectate (1 mM bicuculline or 1 mM strychnine) for post hoc confirmation of injection sites. Control microinjections of equal volumes of the vehicle solution with 0.2% Fast Green dye were also made.

Histology. Injection sites were localized in brainstems fixed (4% formalin in 0.1 M PB, pH 7.4, overnight), cryoprotected with 30% sucrose, frozen, and cut at 20-μm thickness on a cryostat. Coronal sections stained with Cresyl Violet were used for the histological control. Sections were examined in a light and/or epifluorescence microscopy (Eclipse E400 Nikon) equipped with the Nikon Intensilight C-HGFI mercury-fiber illuminator. Photomicrographs and illustrations were performed as described above.

Data analysis. Respiratory frequency (cycles/min), vagal burst duration (ms, measured on raw activity), and peak amplitude of integrated vagal activity (taken as an index of the intensity of vagal bursts, arbitrary units) were measured and averaged for 20 s in the period immediately preceding each trial (control values) and at 2-min intervals during drug application as well as after recovery. Average values of respiratory variables under control conditions, at the time when the maximum response occurred and after recovery were considered for statistical analysis (GraphPad Prism 5). Respiratory responses to each microinjected drug were analyzed by means of the one-way repeated-measures ANOVA, followed by Student–Newman–Keuls tests. One-way ANOVA followed by Student–Newman–Keuls tests was employed to compare changes in respiratory frequency in response to different drugs at the same or at different locations. Changes in respiratory variables were also expressed as percentage variations of control values. The number of preparations employed in each set of drug challenges is indicated by n. All values are mean ± SEM; $P < 0.05$ was considered as significant.

RESULTS

Brainstem afferent projections to the pTRG from the respiratory motoneuron region and the OLA

Unilateral injections of Neurobiotin ($n = 6$) were performed into the pTRG to characterize pTRG afferent projections from the brainstem region extending from the facial to the vagal motor nucleus. One representative preparation was selected to illustrate the distribution of retrogradely labeled neurons on transverse sections of the rhombencephalon, where dots represent ipsi- and contralateral retrogradely labeled cells (Fig. 1). The total number of labeled neurons collected from six preparations in each considered motor region is reported in the histograms of Fig. 2. Retrogradely labeled neurons were both ipsi- and contralateral to the pTRG injections, although the majority of them was located on the ipsilateral side. Present results not only confirm the presence of a direct projection from the vagal area to the pTRG (Cinelli et al., 2014), but also indicate that projecting neurons formed a continuum extending from the facial to the vagal level. Cells were found either intermingled with respiratory motoneurons or in close vicinity to them (Fig. 1B–F). Labeled neurons at the level of respiratory motoneuron areas were round or fusiform, and the largest diameter of their soma ranged from 8 to 25 μm (17.5 ± 0.42 μm) measured on 113 cells in one preparation. As shown in Fig. 1B–D, Neurobiotin injections into the pTRG also labeled a population of similar neurons in a periventricular cell layer of the OLA on both the ipsi- and contralateral side (Fig. 2). Owing to the relatively small number of retrogradely labeled neurons, they were counted on transverse sections of the entire OLA, between the VII and the rostral part of the vagal motor nucleus (Fig. 2A). The largest diameter of their soma ranged from 10 to 24 μm (18.2 ± 1.1 μm; measured on 22 cells in one preparation). Examples of Neurobiotin-labeled neurons on both the ipsi- and contralateral side along with the injection site within the pTRG are shown in Fig. 2B–I. Unilateral injections in the pTRG also confirmed the presence of cross-connections between the two pTRGs (Gariépy et al., 2012a) by showing many small to medium-sized labeled neurons in the contralateral pTRG (Fig. 2C). The largest diameters of their soma ranged from 10 to 22 μm (16.2 ± 0.33 μm; measured on 25 cells in one preparation).

Distribution of glutamate, glycine and GABA immunoreactivity within the respiratory motoneuron region

The presence of glutamate, glycine and GABA immunoreactivity was investigated by double-labeling experiments within the respiratory motoneuron region. Examples of the results obtained in the vagal motoneuron region are illustrated in Fig. 3. Immunohistochemistry showed that retrogradely labeled neurons were immunoreactive for glutamate (Fig. 3A–C). However, also some unlabeled neurons displayed glutamate immunoreactivity. Furthermore, it was found that glycine-immunoreactive neurons were located in the vicinity of retrogradely labeled neurons (Fig. 3D–F). The green neurons in Fig. 3E constitute a dense population of small glycinergic neurons mainly located in an area encompassing the lower border of the vagal nucleus. The motoneurons have a much larger size, do not express glycine-immunoreactivity and, although not clearly visible in Fig. 3E, they are located in part intermingled with glycinergic cells and in part in the upper side of the approximate X profile indicated by the dotted line. Although glycine-immunoreactive cells could be clearly distinguished from background fluorescence by their intense labeling, glycine-immunoreactive structures surrounding retrogradely labeled neurons or in close apposition to them could not be appreciated. Immunohistochemistry also showed that almost all retrogradely labeled neurons were surrounded by intense GABA immunoreactivity (Fig. 3G–I). The inset at higher magnification reveals small GABA-immunoreactive structures, probably synaptic terminals, in close apposition to retrogradely labeled cells. Despite that a few GABA-immunoreactive neurons were found within or the vicinity of the respiratory motoneuron region, they were not seen in the vicinity of retrogradely labeled neurons. Facial and glossopharyngeal motoneuron regions displayed similar immunohistochemical features (not shown).

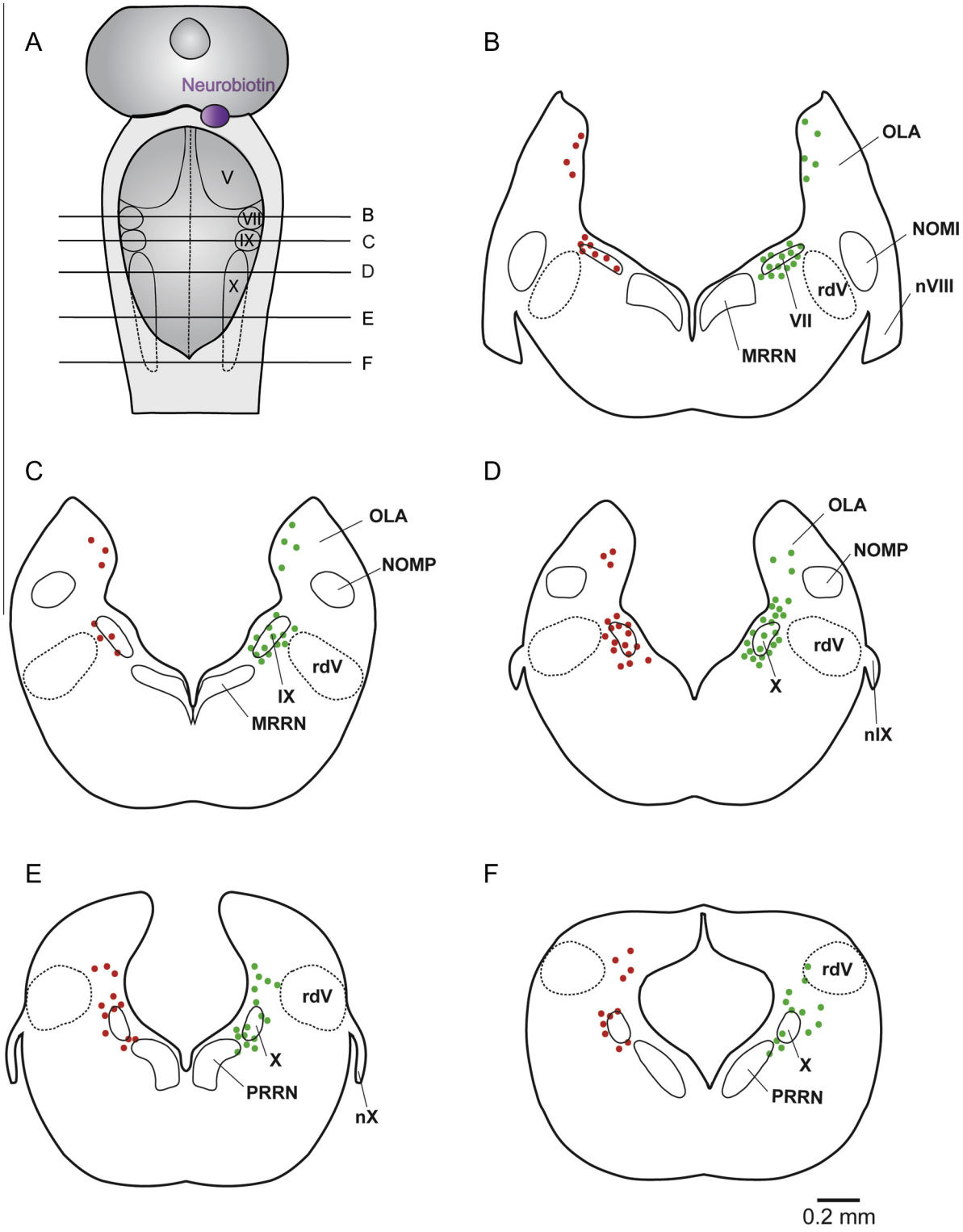

Fig. 1. Distribution of retrogradely labeled neurons. (A) Schematic illustration of a dorsal view of the lamprey mesencephalon/rhombencephalon showing the levels of the transverse sections illustrated in B–F (unbroken lines) and the location of the Neurobiotin injection (pink area). (B–F) Schematic drawings of transverse sections of the lamprey rhombencephalon illustrating the distribution of retrogradely labeled neurons after an injection of Neurobiotin into the pTRG (ipsilateral side, green dots; contralateral side, red dots; data from a representative preparation). The drawings are arranged from rostral (B) to caudal (F). MRRN, middle rhombencephalic reticular nucleus; NOMI, intermediate octavomotor nucleus; NOMP, posterior octavomotor nucleus; nVIII, vestibular nerve; nIX, glossopharyngeal nerve; nX, vagal nerve; OLA, octavolateral area; PRRN, posterior rhombencephalic reticular nucleus; rdV, descending root of the trigeminal nerve; V, trigeminal motor nucleus; VII, facial motor nucleus; IX, glossopharyngeal motor nucleus; X, vagal motor nucleus. (For interpretation of the references to colour in this figure legend, the reader is referred to the web version of this article.)

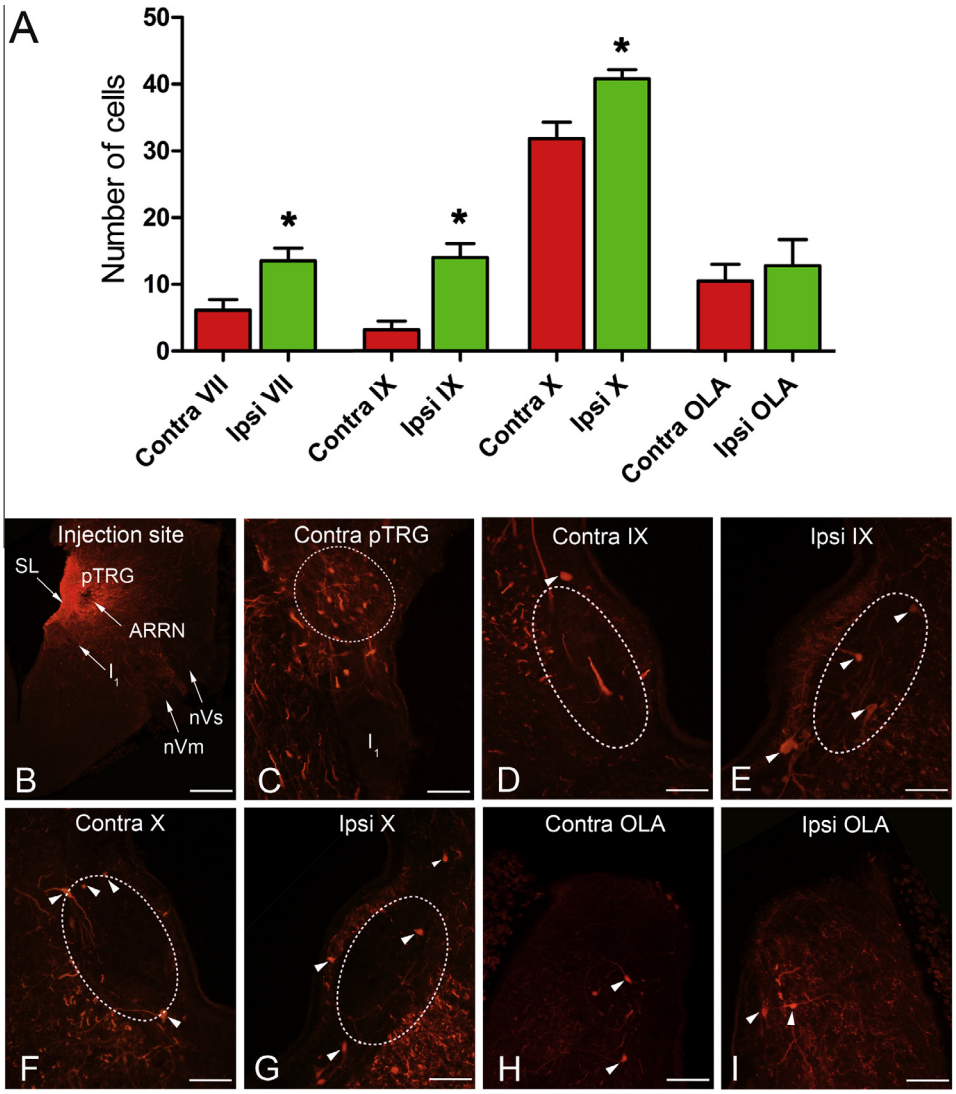

Fig. 2. Retrogradely labeled neurons in the rhombencephalon of the lamprey after unilateral injections of Neurobiotin into the pTRG. (A) The distribution of retrogradely labeled neurons (six preparations) in the respiratory motoneuron regions and octavolateral area (OLA) is illustrated by histograms. Values are mean ± SEM; $^{*}P < 0.05$. (B) Photomicrograph of a transverse section of the isthmic region showing the site of a Neurobiotin injection into the pTRG. (C) Photomicrograph of a transverse section of the isthmic region showing retrogradely labeled neurons (red signal) within the contralateral pTRG (dotted line). (D, E) Photomicrographs of transverse sections of the contralateral and ipsilateral glossopharyngeal (IX) motoneuron region (dotted line) showing retrogradely labeled neurons (red signal). (F, G) Photomicrographs of transverse sections of the contralateral and ipsilateral vagal (X) motoneuron region (dotted line) showing retrogradely labeled neurons (red signal). (H, I) Photomicrographs of transverse sections of the contralateral and ipsilateral OLA in the alar plate at the level of the rostral part of the vagal nucleus showing retrogradely labeled neurons (red signal). Arrowheads point to some retrogradely labeled neurons. ARRN, anterior rhombencephalic reticular nucleus; I_1, isthmic Müller cell; pTRG, paratrigeminal respiratory group; SL, sulcus limitans of His; nVm, motor root of the trigeminal nerve; nVs, sensory root of the trigeminal nerve. Scale bars (B): 200 μm; (C–I): 100 μm. (For interpretation of the references to color in this figure legend, the reader is referred to the web version of this article.)

Distribution of glutamate, glycine and GABA immunoreactivity within the OLA

Since Neurobiotin injections into the pTRG also labeled a population of neurons within the OLA, we sought to examine the presence of glutamate, glycine and GABA immunoreactivity within this region by double-labeling experiments. The distribution of glutamate, glycine and GABA immunoreactivity within the OLA displayed similar features at all the investigated levels. Examples of the results are illustrated in Fig. 4. The majority of labeled neurons displayed glutamatergic immunoreactivity (Fig. 4A–C). Glycine-immunoreactive neurons were found to be located within the same region containing retrogradely labeled neurons (Fig. 4D–F). Finally, retrogradely labeled neurons were surrounded by intense GABA immunoreactivity (Fig. 4G–I). The inset at higher magnification shows small GABA-immunoreactive dots, probably synaptic terminals, in close apposition to retrogradely labeled neurons. GABA-immunoreactive neurons were present in the periventricular cell layer of the OLA, also relatively close to the retrogradely labeled neurons.

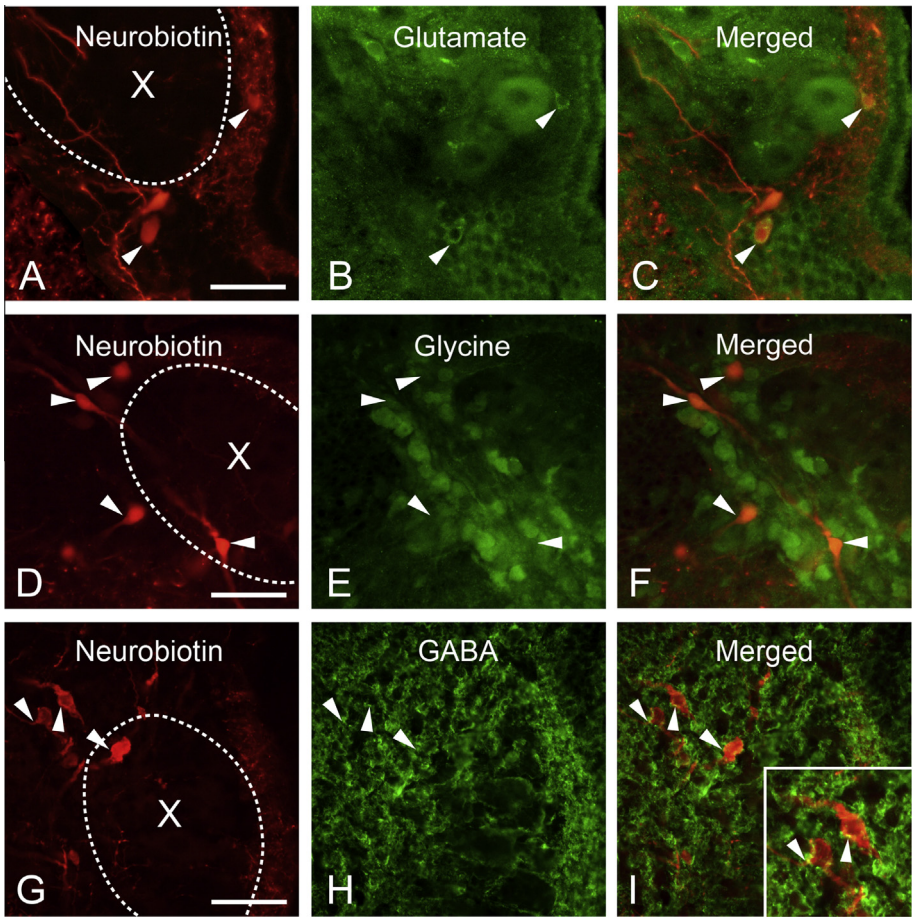

Fig. 3. Distribution of glutamate, glycine and GABA immunoreactivity in the vagal motoneuron region. (A–C) Photomicrographs of a transverse section showing retrogradely labeled neurons (A, red signal) after a Neurobiotin injection into the pTRG, glutamate immunoreactivity (B, green signal) and merged image (C). Retrogradely labeled neurons displaying immunoreactivity for glutamate are indicated by arrowheads. (D–F) Photomicrographs of a transverse section showing retrogradely labeled neurons (D, red signal) after an injection of Neurobiotin into the pTRG, glycine immunoreactivity (E, green signal) and merged image (F). Retrogradely labeled neurons located in close vicinity of glycinergic neurons are indicated by arrowheads. (G–I) Photomicrographs of a transverse section showing retrogradely labeled neurons (G, red signal) after an injection of Neurobiotin into the pTRG, GABA immunoreactivity (H, green signal) and merged image (I). Retrogradely labeled neurons displaying close apposition of GABA-immunoreactive structures are indicated by arrowheads. The inset (1.5× magnification) shows small GABA-immunoreactive structures, probably synaptic terminals, in close apposition to retrogradely labeled cells (arrowheads). Scale bar = 50 μm. (For interpretation of the references to color in this figure legend, the reader is referred to the web version of this article.)

Role of $GABA_A$ and glycine receptors within the respiratory motoneuron region and the OLA

To extend our previous results (Cinelli et al., 2014) on the involvement of retrogradely labeled neurons within the respiratory motoneuron regions in the regulation of the respiratory frequency, bilateral microinjections of bicuculline or strychnine were performed into these regions. Microinjections of 1 mM bicuculline (0.5–1 pmol; $n = 5$) and 1 mM strychnine (0.5–1 pmol; $n = 5$) into the vagal motoneuron region caused increases in respiratory frequency from 61.4 ± 2.2 to 88.2 ± 2.8 cycles/min ($P < 0.001$) and from 62.0 ± 2.8 to 84.6 ± 2.5 cycles/min ($P < 0.001$), respectively (Fig. 5A). Excitatory effects on respiratory activity were obtained following microinjections of both 1 mM bicuculline ($n = 5$; from 60.5 ± 4.3 to 71.8 ± 4.5 cycles/min; $P < 0.05$) and 1 mM strychnine ($n = 5$; from 60.2 ± 1.8 to 71.2 ± 3.3 cycles/min; $P < 0.05$) into the region of glossopharyngeal motoneurons (Fig. 5B). Bilateral microinjections of bicuculline and strychnine were performed into the OLA to also verify whether GABAergic and glycinergic inputs to retrogradely labeled neurons within this region were involved in the control of the respiratory frequency. Microinjections of 1 mM bicuculline (0.5–1 pmol; $n = 5$) and 1 mM strychnine (0.5–1 pmol; $n = 5$) into the OLA at the level of the rostral part of the vagal nucleus induced increases in respiratory frequency from 60.4 ± 3.4 to 89.8 ± 4.7 cycles/min ($P < 0.001$) and from 60.5 ± 4.1 to 82.9 ± 4.9 cycles/min ($P < 0.001$), respectively (Fig. 6A). Increases in respiratory frequency were also obtained following microinjections of 1 mM bicuculline ($n = 5$; from 60.9 ± 2.8 to 86.7 ± 3.3 cycles/min; $P < 0.001$) and 1 mM strychnine ($n = 5$; from 57.6 ± 4.1 to 78.5 ± 4.8 cycles/min; $P < 0.001$) into the region of OLA at the level of the glossopharyngeal nucleus (Fig. 6B). Statistical comparisons are presented in Table 1 where data are expressed as percentage of control values. Respiratory changes obtained in response to bicuculline

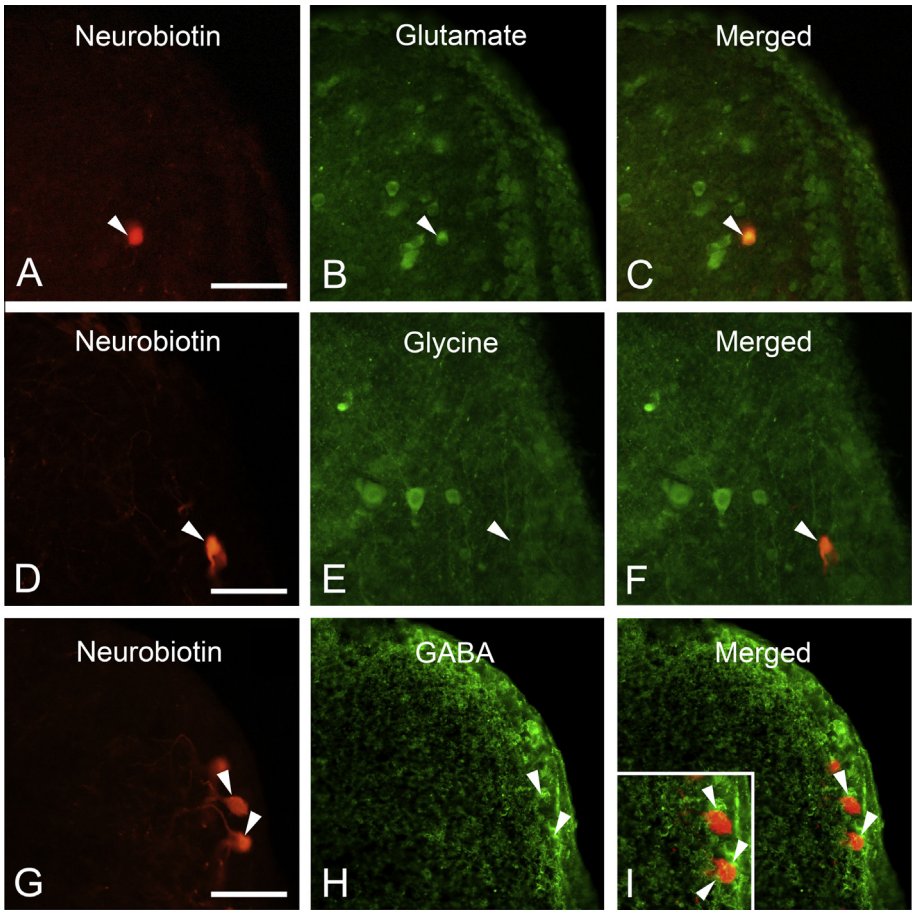

Fig. 4. Distribution of glutamate, glycine and GABA immunoreactivity in the OLA. (A–C) Photomicrographs of a transverse section showing a retrogradely labeled neuron (A, red signal) within the OLA at the rostral level of the vagal region after an injection of Neurobiotin into the pTRG, glutamate immunoreactivity (B, green signal) and merged image (C). The retrogradely labeled neuron displaying immunoreactivity for glutamate is indicated by an arrowhead. (D–F) Photomicrographs of a transverse section showing a retrogradely labeled neuron (D, red signal) within the OLA at the glossopharyngeal level after an injection of Neurobiotin into the pTRG, glycine immunoreactivity (E, green signal) and merged image (F). The retrogradely labeled neuron (arrowhead) is associated with the presence of glycinergic neurons. (G–I) Photomicrographs of a transverse section showing retrogradely labeled neurons (G, red signal) within the OLA at the facial level after an injection of Neurobiotin into the pTRG, GABA immunoreactivity (H, green signal) and merged image (I). Retrogradely labeled neurons showing close apposition of GABA-immunoreactive structures are indicated by arrowheads. The inset (1.5× magnification) shows GABA-immunoreactive structures, probably synaptic terminals, in close apposition to retrogradely labeled cells (arrowheads). Scale bar = 50 μm. (For interpretation of the references to color in this figure legend, the reader is referred to the web version of this article.)

or strychnine at both the OLA levels were similar to those evoked by microinjections of the same drugs into the vagal region, but more intense than those obtained at the glossopharyngeal level. In all instances, the duration and amplitude of vagal bursts did not change; the respiratory responses reached a maximum within ~4 min, while the recovery occurred within 20 min. Representative examples of the time courses concerning only bicuculline-induced respiratory effects in the investigated regions are reported in Fig. 7.

The localization of 1 mM bicuculline microinjections within the respiratory motoneuron column is illustrated in Fig. 5C, D. It should be noted that the spread of the injectate into the glossopharyngeal motoneuron region also involved the strictly contiguous facial motoneuron region (Fig. 5D). Localizations of bicuculline injections within the OLA at the level of the vagal and glossopharyngeal regions are illustrated in Fig. 6A, B. Microinjections aimed at selectively affecting only the region of the facial nucleus or the portion of the OLA at the same level were not attempted. In each responsive site, control microinjections (3 trials) of equivalent volumes of the vehicle solution containing 0.2% Fast Green did not cause any obvious respiratory response.

Respiratory responses caused by the activation or blockade of OLA neurons

To further characterize the respiratory role of the OLA, some drugs were bilaterally microinjected into this neural structure at the level of the glossopharyngeal motor nucleus. Since OLA neurons displayed similar functional and immunohistochemical characteristics at all the investigated levels, the responses to microinjections into the OLA at this level were taken as representative of the entire area. Microinjections (n = 4) of a mixture of the glutamate agonists AMPA (1 mM, 0.5–1 pmol) and NMDA (2 mM, 1–2 pmol) increased the

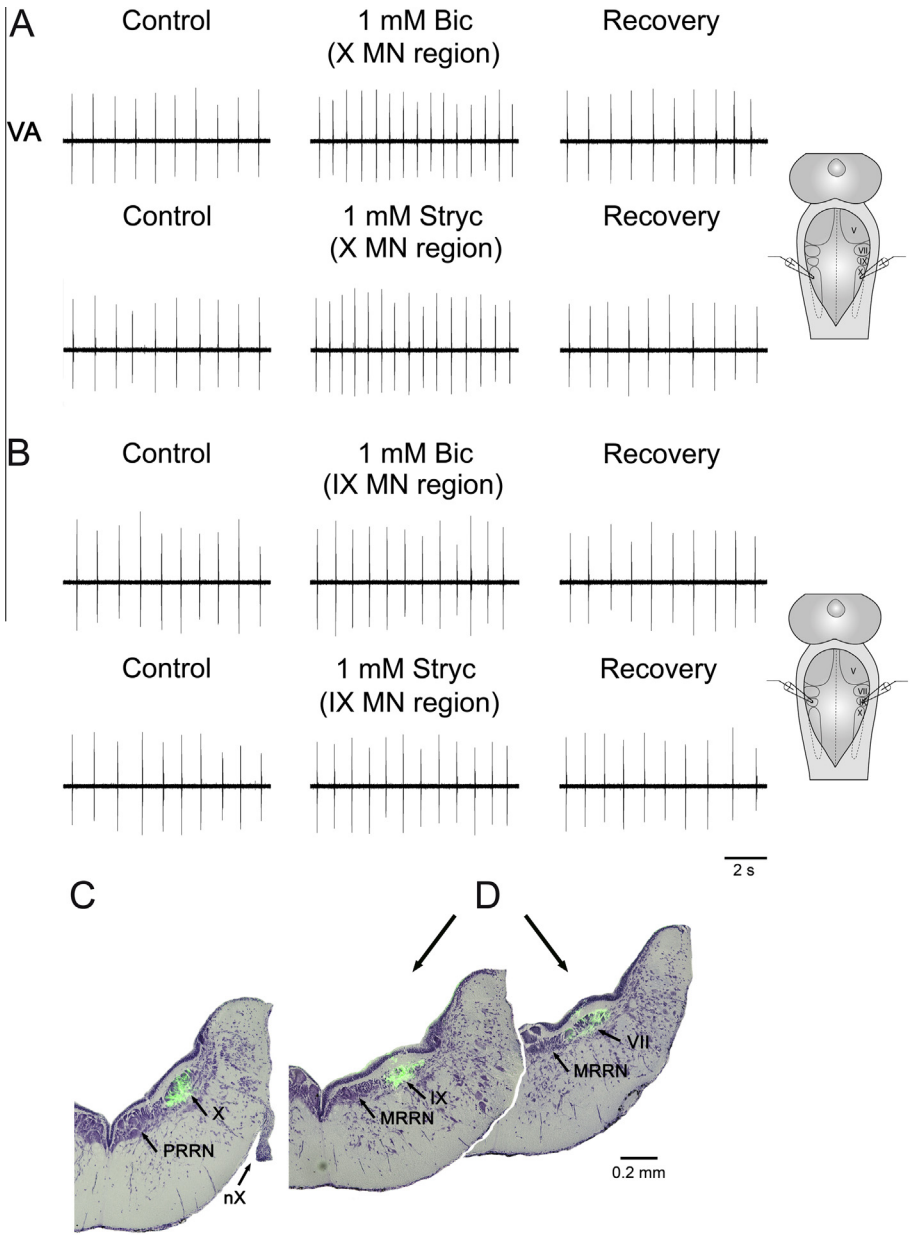

Fig. 5. Respiratory responses to bicuculline and strychnine microinjections into the respiratory motoneuron column. (A) Marked increases in respiratory frequency ~4 min after bilateral microinjections of 1 mM bicuculline (Bic) or 1 mM strychnine (Stryc) into the region of vagal motoneurons (X MN region). (B) Increases in respiratory frequency ~4 min after bilateral microinjections of 1 mM bicuculline (Bic) or 1 mM strychnine (Stryc) into the region of glossopharyngeal motoneurons (IX MN region). The sites where Bic or Stryc were microinjected are shown on a schematic illustration of a dorsal view of the lamprey mesencephalon/rhombencephalon. (C, D) Photomicrographs of transverse sections of the rhombencephalon showing the location of the fluorescent beads (green) added to 1 mM bicuculline microinjected into the vagal motoneuron region (C) and into the glossopharyngeal motoneuron region (D). Note that the spread of the fluorescent beads microinjected into the glossopharyngeal motoneuron region also involves the closely located region of facial motoneurons (D). Sections are counterstained with Cresyl Violet. Light-field and fluorescence photomicrographs have been superimposed. MRRN, middle rhombencephalic reticular nucleus; nX, vagal nerve; PRRN, posterior rhombencephalic reticular nucleus; V, trigeminal motor nucleus; VII, facial motor nucleus; IX, glossopharyngeal motor nucleus; X, vagal motor nucleus; VA, raw vagal nerve activity. (For interpretation of the references to colour in this figure legend, the reader is referred to the web version of this article.)

respiratory frequency from 63.5 ± 2.9 to 82.2 ± 3.7 cycles/min (29.5 ± 2.1%; $P < 0.01$) without significant changes in the duration and amplitude of vagal bursts (Fig. 8A). The respiratory responses reached a maximum within 2 min and the recovery was observed within 20 min. On the other hand, the blockade of glutamate receptors within the OLA by means of microinjections ($n = 3$) of a mixture of 1 mM CNQX (0.5–1 pmol) and 5 mM D-AP5 (2.5–5 pmol) did not cause any obvious respiratory effect (Fig. 8B). Similarly, microinjections of 0.2 mM muscimol (0.1–0.2 pmol; $n = 3$) failed to induce any change in respiratory activity (Fig. 8C).

DISCUSSION

The results provide evidence that neurons retrogradely labeled by injections of Neurobiotin into the pTRG do

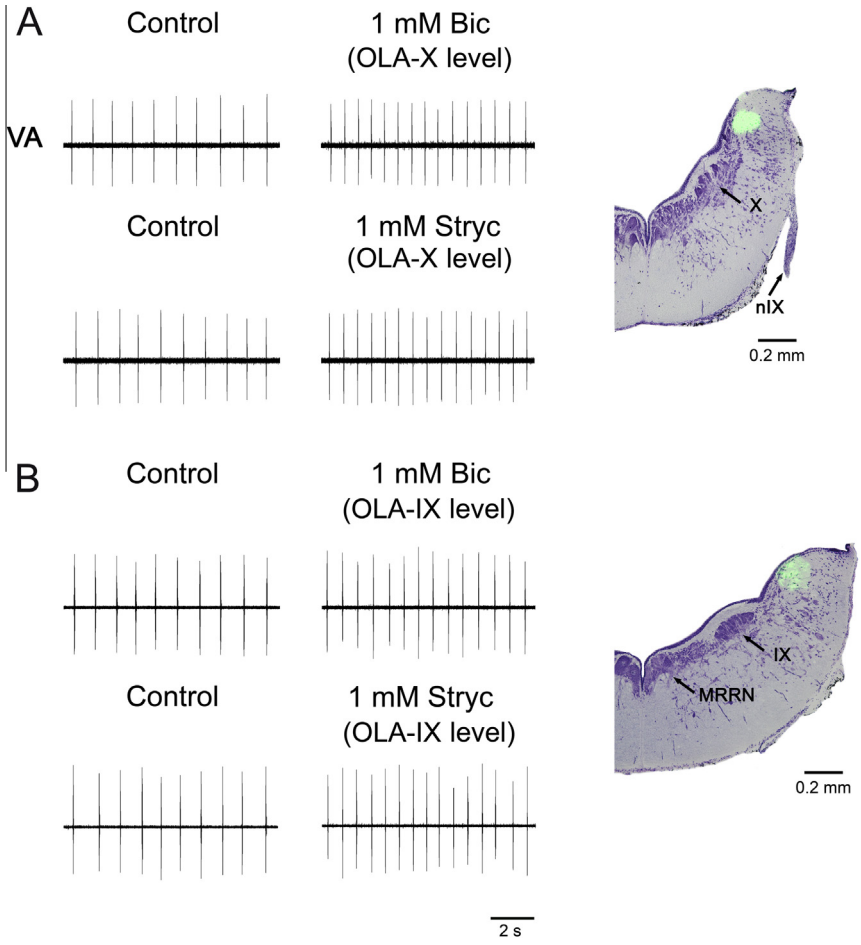

Fig. 6. Respiratory responses to bicuculline and strychnine microinjections into the OLA. (A) Increases in respiratory frequency ~4 min after bilateral microinjections of 1 mM bicuculline (Bic) or 1 mM strychnine (Stryc) into the OLA at the rostral level of the vagal region (OLA-X level). (B) Increases in respiratory frequency ~4 min after bilateral microinjections of 1 mM bicuculline (Bic) or 1 mM strychnine (Stryc) into the OLA at the glossopharyngeal level (OLA-IX level). Photomicrographs of transverse sections of the rhombencephalon showing the location of the fluorescent beads (green) added to 1 mM bicuculline microinjected into the OLA are shown on the right panels in A and B. Sections counterstained with Cresyl Violet. Light-field and fluorescence photomicrographs have been superimposed. MRRN, middle rhombencephalic reticular nucleus; nIX, glossopharyngeal nerve; IX, glossopharyngeal motor nucleus; X, vagal motor nucleus; VA, raw vagal nerve activity. (For interpretation of the references to color in this figure legend, the reader is referred to the web version of this article.)

exist not only at the level of the vagal nucleus, but also within the glossopharyngeal and facial regions. In addition, the present study is the first to also reveal that the OLA is involved in the regulation of the respiratory frequency through an ascending excitatory pathway controlled by potent inhibitory inputs. A striking finding is that projecting neurons are immunoreactive for glutamate, surrounded by GABAergic structures and associated with the presence of glycinergic cells. Interestingly, like the respiratory motor region, also the OLA does not contribute to respiratory rhythm generation, but can produce increases in respiratory frequency when its neurons are activated or disinhibited.

Ascending excitatory projections from the respiratory motoneuron region to the pTRG

Labeled cells were distributed bilaterally with an ipsilateral dominance along the caudorostral extent of the basal plate at the level of vagal, glossopharyngeal and facial motor nuclei. The results extend our previous findings concerning only the vagal motoneuron region (Cinelli et al., 2014). All labeled neurons have similar morphological characteristics. They are arranged in an almost continuous column and can be distinguished from branchial motoneurons by large differences in size and morphology (see also Rovainen, 1974; Guimond et al., 2003; Bongianni et al., 2016). We are confident that Neurobiotin injections were performed into the pTRG in agreement with the anatomical landmarks previously described, i.e. they were localized in a dorsal aspect of the anterior rhombencephalic reticular nucleus (ARRN), at the level of the I_1 and close to the SL. (Mutolo et al., 2007, 2010, 2011; Cinelli et al., 2013, 2014; Bongianni et al., 2016). Consistently with previous results (Gariépy et al., 2012a), small to medium-sized retrogradely labeled neurons were found in the contralateral pTRG (see also Bongianni et al., 2016). Reciprocal connections between

Table 1. Changes in respiratory frequency after bilateral bicuculline and strychnine microinjections

	Respiratory frequency (percentages of control values)	
	1 mM Bicuculline	1 mM Strychnine
X MN region $n = 5$	+44.0 ± 6.3	+36.7 ± 3.6
IX MN region $n = 5$	+19.0 ± 3.6*,#,§	+18.0 ± 2.2*,#,§
OLA-X level $n = 5$	+49.5 ± 5.5	+37.8 ± 4.6
OLA-IX level $n = 5$	+43.0 ± 6.1	+36.8 ± 2.8

Data (percentage of control values) are mean ± SEM; *n*, number of animals. X MN region, vagal motoneuron region; IX MN region, glossopharyngeal motoneuron region; OLA-X level, octavolateral area at the level of the rostral part of the vagal nucleus; OLA-IX level, octavolateral area at the level of the glossopharyngeal nucleus. No significant differences were found between the effects of bicuculline and strychnine in all the investigated regions. Only drug-induced increases in respiratory frequency in the IX MN region turned out to be significantly different from those obtained in the other regions.

* $P < 0.05$ compared with bicuculline or strychnine microinjections into the X MN region.

# $P < 0.05$ compared with bicuculline or strychnine microinjections into the OLA-X region.

§ $P < 0.05$ compared with bicuculline or strychnine microinjections into the OLA-IX region.

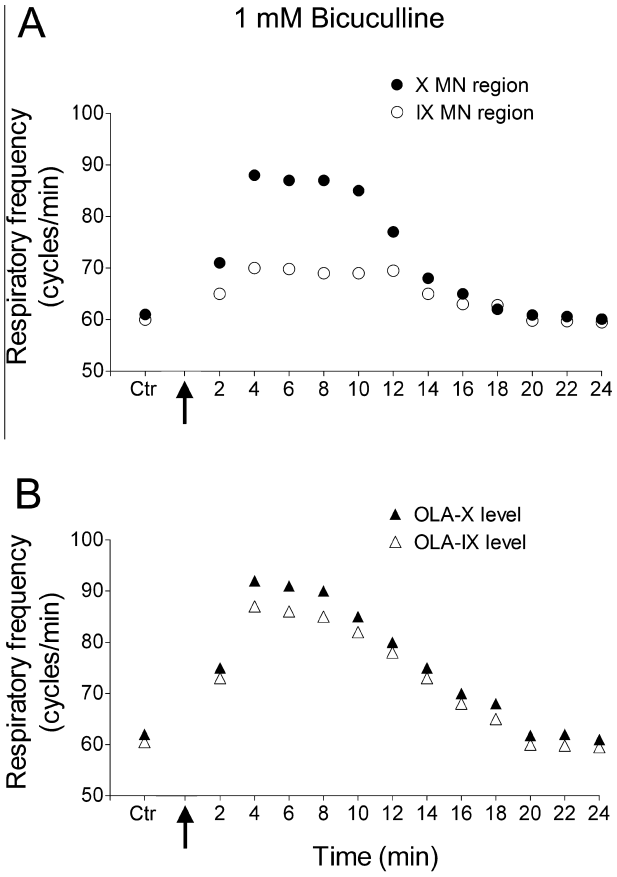

Fig. 7. Examples of the time courses of bicuculline-induced effects on the respiratory frequency. (A) Microinjections performed into the vagal motoneuron region (X MN region) and the glossopharyngeal motoneuron region (IX MN region). (B) Microinjections performed into the OLA at the rostral level of the vagal region (OLA-X level) and at the glossopharyngeal level (OLA-IX level). Microinjections indicated by arrows. Data are derived from four different preparations.

the two pTRGs along with the bilateral ascending projections to the pTRG may account for the bilateral effects obtained by unilateral microinjections into the respiratory motoneuron regions (see Cinelli et al., 2014).

Microinjections of bicuculline or strychnine into the region of glossopharyngeal motor region caused increases in respiratory frequency, although less intense than those elicited by similar microinjections into the vagal motoneuron region or the OLA. The reasons for these findings are not obvious. Differences in the density of retrogradely labeled neurons as well as in the intensity of the inhibitory control and in the strength of excitatory synapses at the level of the pTRG could have played a role. However, at present evidences supporting this view are not available. As already discussed (Cinelli et al., 2014), the respiratory effects caused by the blockade of inhibitory transmission within the respiratory motor column do not appear to be due to a direct action on the respiratory motoneurons since they were not retrogradely labeled from the pTRG. On the other hand, we have also shown that respiratory motoneurons do not have *per se* rhythmogenic properties, but seem to represent merely an output system (Cinelli et al., 2014). Furthermore, in all instances the duration and amplitude of vagal bursts did not change. This appears to imply that inhibitory neurons do not affect the activity of respiratory motoneurons in agreement with the results of previous studies (Rovainen, 1983; Cinelli et al., 2014).

The present study demonstrates that retrogradely labeled neurons are immunoreactive for glutamate showing that glutamatergic transmission mediates the excitatory ascending inputs to pTRG neurons. The finding that numerous glutamatergic neurons are present in the basal plate of the lamprey brainstem in the vicinity of respiratory motoneurons (Villar-Cerviño et al., 2013) is consistent with present results. The respiratory responses obtained following blockade of GABAergic and glycinergic neurotransmission within these regions are corroborated by the results on GABA and glycine immunoreactivity. Present findings on GABA and glycine immunoreactivity within the respiratory motor column of the lamprey are in agreement with previous results (Robertson et al., 2007; Villar-Cerviño et al., 2008). In this study, evidence has been provided that retrogradely labeled neurons are surrounded by GABA immunoreactivity and that GABA-immunoreactive structures are in close apposition to these cells, suggesting the presence of synaptic terminals. On the contrary, contacts between glycinergic terminals and retrogradely labeled neurons could not be appreciated, since glycinergic cells were strongly labeled, but unfortunately a rather weak fiber staining was obtained. We do not know the reasons for this. In this context, we can recall that the specificity of the rat anti-glycine antibody used has previously been ascertained in a study on the lamprey spinal cord: the rat anti-glycine antibody essentially gave results similar to those obtained with the rabbit anti-glycine antibody (Mahmood et al., 2009). However, we have to acknowledge that immunohistochemical detection

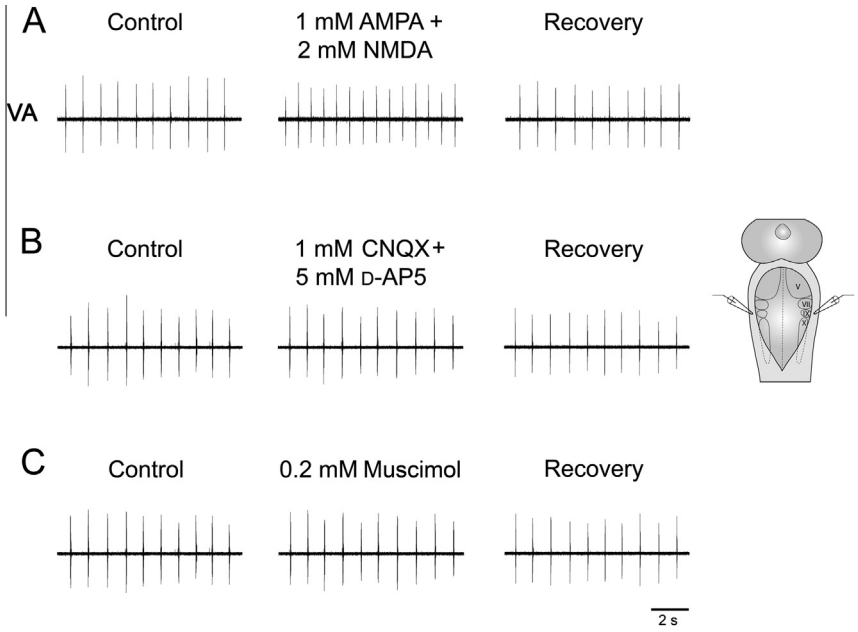

Fig. 8. Examples of respiratory responses evoked by the activation or blockade of OLA neurons. (A) Increases in respiratory frequency ~2 min after bilateral microinjections of a mixture of 1 mM AMPA and 2 mM NMDA into the OLA at the glossopharyngeal level. (B, C) Absence of appreciable respiratory effects ~2 min after bilateral microinjections of 1 mM CNQX/5 mM D-AP5 or 0.2 mM muscimol into the OLA at the same level. Injection sites are shown on a schematic illustration of a dorsal view of the lamprey mesencephalon/rhomboencephalon. V, trigeminal motor nucleus; VII, facial motor nucleus; IX, glossopharyngeal motor nucleus; X, vagal motor nucleus; VA, raw vagal nerve activity.

of glycine is rather difficult in the lamprey and, in our experience, labeling of cell bodies or fiber terminals may strongly depend upon the type and concentration of the fixative employed (see also Rampon et al., 1996; Mahmood et al., 2009). On the other hand, our neuropharmacological experiments clearly show that glycine receptors do exist in the injected area and have a role in the disinhibition of ascending projections. Taken together, our results clearly indicate that GABAergic and glycinergic inputs to neurons located within the respiratory motor nuclei are involved in the regulation of the respiratory frequency via ascending glutamatergic projections to the pTRG.

Ascending excitatory projections from the OLA to the pTRG

Remarkably, Neurobiotin injections into the pTRG also labeled neurons in the alar plate. In particular, retrogradely labeled neurons were found mainly in a periventricular layer at the level of the respiratory motor column. This location could correspond at least in part to that of neurons of the dorsal and medial octavolateral nuclei described in previous studies (Nieuwenhuys, 1972; Northcutt, 1979; Bodznick and Northcutt, 1981; Ronan and Northcutt, 1987; Koyama et al., 1990; Koyama, 2005). As in the respiratory motor regions, retrogradely labeled neurons were both ipsi- and contralateral to the pTRG. Furthermore, they resulted to be immunoreactive for glutamate, to receive GABAergic inputs and to be in association with glycinergic neurons, thus suggesting that also OLA neurons are involved in the respiratory regulation via ascending excitatory projections to the pTRG and are subject to a potent inhibitory control. Accordingly, blockade of GABAergic and glycinergic neurotransmission as well as microinjections of glutamate agonists causes increases in respiratory frequency. In addition, the fact that microinjections of glutamate antagonists or muscimol were ineffective implies that, like the respiratory motor region, the OLA is also not involved in respiratory rhythm generation, but can increase the respiratory frequency when its neurons are brought into action by disinhibition or activation. Our immunohistochemical results concerning the OLA are consistent with previous results (Robertson et al., 2007; Villar-Cerviño et al., 2008, 2013). It can also be mentioned that not only ascending projections from the respiratory motor column, but also those from the OLA could obviously contribute to the respiratory responses obtained by bath application of bicuculline or strychnine (Bongianni et al., 2006).

Functional considerations

The main issues arising from the present results are the source of the inhibitory control of the ascending glutamatergic pathways and that of the inputs responsible for their activation as well as the circumstances under which they are delivered. In an attempt to provide an interpretation we can take into consideration the functional role of the projecting regions and the inputs they receive. In this connection, it should be recalled that the periventricular and intermediate areas located dorsal to the vagal motor nucleus and ventrolateral to the dorsal column nucleus have been proposed as the homologous of the nucleus tractus solitarii (NTS) of other vertebrates (e.g. Pombal et al., 2001; Koyama, 2005; Villar-Cerviño et al., 2013), i.e. the neural aggregate that receives afferent projections from the facial, glossopharyngeal and vagal nerves.

Taking into consideration that at least part of the retrogradely labeled neurons could be located within this region, we can confirm the hypothesis (Cinelli et al., 2014) that the inhibitory control can be exerted at this level by local interneurons or other unidentified inhibitory neuronal aggregates on second-order sensory neurons which, in turn, may influence the respiratory network. This interpretation is consistent with the functional organization of inhibitory modulation of NTS neurons in mammals (e.g. Miyazaki et al., 1999; Ezure and Tanaka, 2004; Kubin et al., 2006; Bailey et al., 2008). The OLA consists of three primary octavolateralis nuclei arranged dorsoventrally which receive multiple sensory inputs. More specifically, it has been described that the dorsal nucleus receives electroreceptive inputs, the medial nucleus receives mechanoreceptive inputs and the ventral nucleus receives vestibular inputs (Rovainen, 1979; Northcutt, 1979; Bodznick and Northcutt, 1981; Ronan and Northcutt, 1987; Koyama et al., 1990 Nieuwenhuys, 1972). Interestingly, it has been reported that afferent projections of the glossopharyngeal and vagal nerves terminate in the OLA, especially in its medial and ventral nuclei (Koyama, 2005). Furthermore, the OLA receives information from light receptors of the tail and is involved in the initiation of locomotion evoked by tail illumination (Ullén et al., 1993; Deliagina et al., 1995). A study on the primary projections of the lateral line nerves, known to mediate photoreception, electroreception and mechanoreception, reported that some fibers were observed within areas other than the OLA and, in particular, within the vagal motoneuron region (Koyama et al., 1990). Admittedly, the functional role of GABAergic and glycinergic inputs to glutamatergic neurons of the basal and alar plate projecting to the pTRG neurons remains unclear. However, in the light of the above reported considerations, it can be tentatively proposed that at least part of the neurons projecting to the pTRG is involved in sensory-mediated respiratory responses, i.e. in adapting respiratory activity to behavioral and environmental conditions.

Afferent input to the investigated regions may also arise from structures within the central nervous system that are known to influence the respiratory activity, such as the neural system that is involved in triggering both locomotion and increases in respiratory activity in response to internal cues in specific behavioral contexts, such as exploration, food seeking, reproduction and defense reaction. These mechanisms rely on supraspinal structures and involve neurons of the mesencephalic locomotor region (Gariépy et al., 2010, 2012b). We cannot exclude that components of this neural system may operate by removing an inhibitory control on both the respiratory motoneuron region and the OLA.

The presence and the functional role of an ascending excitatory pathway from the lower components of the respiratory network to the respiratory rhythm generator have not yet been extensively investigated in mammals. However, some studies have suggested that neurons located in the caudal ventral respiratory group send excitatory projections to more rostral brainstem regions considered to be responsible for respiratory rhythm generation and pattern formation (Bongianni et al., 1994; Cinelli et al., 2012; Jones et al., 2012 also for further Refs.). In addition, we have also recently found that microinjections of bicuculline and strychnine into the caudal NTS produce intense increases in the respiratory frequency in the rabbit (unpublished observations). Accordingly, both the caudal ventral respiratory group and the caudal NTS neurons have been shown to be subject to a potent inhibitory control (see e.g. Miyazaki et al., 1999; Tonkovic-Capin et al., 2001, 2003; Ezure and Tanaka, 2004; Kubin et al., 2006; Bailey et al., 2008).

CONCLUSION

The results demonstrate the presence of glutamatergic neurons with GABAergic synaptic contacts in association with glycinergic cells both in the respiratory motoneuron region and in the OLA. These glutamatergic neurons project to the respiratory rhythm generator and are brought into action by blockade of inhibitory neurotransmission, thus suggesting that disinhibition is of importance in the regulation of respiratory frequency. Evidence for this has been provided by the concomitant increases in the respiratory frequency and the activity of pTRG neurons observed in response to bicuculline microinjections into the vagal motoneuron region (Cinelli et al., 2014). These ascending projections are possibly involved in sensory-mediated respiratory control. Of note, like other neurophysiological features (Ericsson et al., 2011, 2013; Stephenson-Jones et al., 2011, 2012; Grillner and Robertson, 2015), the general characteristics and the basic functional role of inhibitory mechanisms involved in rhythmic activities, such as respiration, appear to be highly conserved throughout evolution. New findings on the lamprey respiratory network may be useful to provide insights into the basic mechanisms of the central rhythm or pattern generators (Grillner, 2006) and hints for further investigations on this topic not only in the lamprey, but also in higher vertebrates, including mammals.

AUTHORS' CONTRIBUTIONS

E.C., D.M., M.C., F.B. conducted the experiments and primary data analysis and developed the experimental design together with T.P. All authors contributed to the evaluation of the data. F.B. wrote the manuscript in consultation with all authors. All authors have approved the final version.

CONFLICT OF INTEREST

The authors declare no conflict of interest.

Acknowledgments—This study was supported by grants from the Ministry of Education, University, and Research of Italy and the A. Menarini United Pharmaceutical Industries. E.C. is supported by a Postdoctoral Fellowship from the Fondazione Internazionale Menarini.

REFERENCES

Bailey TW, Appleyard SM, Jin YH, Andresen MC (2008) Organization and properties of gabaergic neurons in solitary tract nucleus (Nts). J Neurophysiol 99:1712–1722.

Bodznick D, Northcutt RG (1981) Electroreception in lampreys: evidence that the earliest vertebrates were electroreceptive. Science 212:465–467.

Bongianni F, Corda M, Ga Fontana, Pantaleo T (1994) Chemical activation of caudal medullary expiratory neurones alters the pattern of breathing in the cat. J Physiol 474:497–507.

Bongianni F, Deliagina TG, Grillner S (1999) Role of glutamate receptor subtypes in the lamprey respiratory network. Brain Res 826:298–302.

Bongianni F, Mutolo D, Carfi M, Pantaleo T (2002) Group I and II metabotropic glutamate receptors modulate respiratory activity in the lamprey. Eur J Neurosci 16:454–460.

Bongianni F, Mutolo D, Nardone F, Pantaleo T (2006) Gabaergic and glycinergic inhibitory mechanisms in the lamprey respiratory control. Brain Res 1090:134–145.

Bongianni F, Mutolo D, Cinelli E, Pantaleo T (2016) Neural mechanisms underlying respiratory rhythm generation in the lamprey. Respir Physiol Neurobiol 224:17–26.

Cinelli E, Bongianni F, Pantaleo T, Mutolo D (2012) Modulation of the cough reflex by GABA(A) receptors in the caudal ventral respiratory group of the rabbit. Front Physiol 3:403.

Cinelli E, Robertson B, Mutolo D, Grillner S, Pantaleo T, Bongianni F (2013) Neuronal mechanisms of respiratory pattern generation are evolutionary conserved. J Neurosci 33:9104–9112.

Cinelli E, Mutolo D, Robertson B, Grillner S, Contini M, Pantaleo T, Bongianni F (2014) Gabaergic and glycinergic inputs modulate rhythmogenic mechanisms in the lamprey respiratory network. J Physiol 592:1823–1838.

Deliagina T, Ullén F, Gonzalez M, Ehrsson H, Orlovsky G, Grillner S (1995) Initiation of locomotion by lateral line photoreceptors in lamprey: behavioural and neurophysiological studies. J Exp Biol 198:2581–2591.

Ericsson J, Silberberg G, Robertson B, Wikström MA, Grillner S (2011) Striatal cellular properties conserved from lampreys to mammals. J Physiol 589:2979–2992.

Ericsson J, Stephenson-Jones M, Kardamakis A, Robertson B, Silberberg G, Grillner S (2013) Evolutionarily conserved differences in pallial and thalamic short-term synaptic plasticity in striatum. J Physiol 591:859–874.

Ezure K, Tanaka I (2004) Gaba, in some cases together with glycine, is used as the inhibitory transmitter by pump cells in the Hering-Breuer reflex pathway of the rat. Neuroscience 127:409–417.

Gariépy JF, Missaghi K, Dubuc R (2010) The interactions between locomotion and respiration. Prog Brain Res 187:173–188.

Gariépy JF, Missaghi K, Chartre S, Robert M, Auclair F, Dubuc R (2012a) Bilateral connectivity in the brainstem respiratory networks of lampreys. J Comp Neurol 520:1442–1456.

Gariépy JF, Missaghi K, Chevallier S, Chartre S, Robert M, Auclair F, Lund JP, Dubuc R (2012b) Specific neural substrate linking respiration to locomotion. Proc Natl Acad Sci USA 109:E84–E92.

Grillner S (2006) Biological pattern generation: the cellular and computational logic of networks in motion. Neuron 52:751–766.

Grillner S, Robertson B (2015) The basal ganglia downstream control of brainstem motor centres–an evolutionarily conserved strategy. Curr Opin Neurobiol 33:47–52.

Guimond JC, Auclair F, Lund JP, Dubuc R (2003) Anatomical and physiological study of respiratory motor innervation in lampreys. Neuroscience 122:259–266.

Jones SE, Saad M, Lewis DI, Subramanian HH, Dutschmann M (2012) The nucleus retroambiguus as possible site for inspiratory rhythm generation caudal to obex. Respir Physiol Neurobiol 180:305–310.

Koyama H (2005) Organization of the sensory and motor nuclei of the glossopharyngeal and vagal nerves in lampreys. Zoolog Sci 22:469–476.

Koyama H, Kishida R, Rc Goris, Kusunoki T (1990) Organization of the primary projections of the lateral line nerves in the lamprey Lampetra japonica. J Comp Neurol 295:277–289.

Kubin L, Alheid GF, Zuperku EJ, Mccrimmon DR (2006) Central pathways of pulmonary and lower airway vagal afferents. J Appl Physiol 101:618–627.

Kumar S, Hedges SB (1998) A molecular timescale for vertebrate evolution. Nature 392:917–920.

Mahmood R, Restrepo CE, El Manira A (2009) Transmitter phenotypes of commissural interneurons in the lamprey spinal cord. Neuroscience 164:1057–1067.

Martel B, Guimond JC, Gariepy JF, Gravel J, Auclair F, Kolta A, Lund JP, Dubuc R (2007) Respiratory rhythms generated in the lamprey rhombencephalon. Neuroscience 148:279–293.

Miyazaki M, Tanaka I, Ezure K (1999) Excitatory and inhibitory synaptic inputs shape the discharge pattern of pump neurons of the nucleus tractus solitarii in the rat. Exp Brain Res 129:191–200.

Mutolo D, Bongianni F, Einum J, Dubuc R, Pantaleo T (2007) Opioid-Induced depression in the lamprey respiratory network. Neuroscience 150:720–729.

Mutolo D, Bongianni F, Cinelli E, Pantaleo T (2010) Role of neurokinin receptors and ionic mechanisms within the respiratory network of the lamprey. Neuroscience 169:1136–1149.

Mutolo D, Cinelli E, Bongianni F, Pantaleo T (2011) Identification of a cholinergic modulatory and rhythmogenic mechanism within the lamprey respiratory network. J Neurosci 31:13323–13332.

Nieuwenhuys R (1972) Topological analysis of the brain stem of the lamprey *Lampetra fluviatilis*. J Comp Neurol 145:165–177.

Northcutt RG (1979) Central projections of the eighth cranial nerve in lampreys. Brain Res 167:163–167.

Pombal MA, Marin O, Gonzalez A (2001) Distribution of choline acetyltransferase-immunoreactive structures in the lamprey brain. J Comp Neurol 431:105–126.

Rampon C, Luppi PH, Fort P, Peyron C, Jouvet M (1996) Distribution of glycine-immunoreactive cell bodies and fibers in the rat brain. Neuroscience 75:737–755.

Robertson B, Auclair F, Ménard A, Grillner S, Dubuc R (2007) Gaba distribution in lamprey is phylogenetically conserved. J Comp Neurol 503:47–63.

Ronan M, Northcutt RG (1987) Primary projections of the lateral line nerves in adult lampreys. Brain Behav Evol 30:62–81.

Rovainen CM (1974) Respiratory motoneurons in lampreys. J Comp Physiol 94:57–68.

Rovainen CM (1977) Neural control of ventilation in the lamprey. Fed Proc 36:2386–2389.

Rovainen CM (1979) Neurobiology of lampreys. Physiol Rev 59:1007–1077.

Rovainen CM (1983) Generation of respiratory activity by the lamprey brain exposed to picrotoxin and strychnine, and weak synaptic inhibition in motoneurons. Neuroscience 10:875–882.

Russell DF (1986) Respiratory pattern generation in adult lampreys (*Lampetra fluviatilis*): interneurons and burst resetting. J Comp Physiol A 158:91–102.

Stephenson-Jones M, Samuelsson E, Ericsson J, Robertson B, Grillner S (2011) Evolutionary conservation of the basal ganglia as a common vertebrate mechanism for action selection. Curr Biol 21:1081–1091.

Stephenson-Jones M, Ericsson J, Robertson B, Grillner S (2012) Evolution of the basal ganglia; dual output pathways conserved throughout vertebrate phylogeny. J Comp Neurol 520:2957–2973.

Thompson KJ (1985) Organization of inputs to motoneurons during fictive respiration in the isolated lamprey brain. J Comp Physiol A 157:291–302.

Tonkovic-Capin V, Stucke AG, Stuth EA, Tonkovic-Capin M, Krolo M, Hopp FA, Mccrimmon DR, Zuperku EJ (2001) Differential modulation of respiratory neuronal discharge patterns by Gaba (A) receptor and apamin-sensitive K(+) channel antagonism. J Neurophysiol 86:2363–2373.

Tonkovic-Capin V, Stucke AG, Stuth EA, Tonkovic-Capin M, Hopp FA, Mccrimmon DR, Zuperku EJ (2003) Differential processing of

excitation by gabaergic gain modulation in canine caudal ventral respiratory group neurons. J Neurophysiol 89:862–870.

Ullén F, Orlovsky GN, Deliagina TG, Grillner S (1993) Role of dermal photoreceptors and lateral eyes in initiation and orientation of locomotion in lamprey. Behav Brain Res 54:107–110.

Villar-Cerviño V, Barreiro-Iglesias A, Anadón R, Mc Rodicio (2008) Distribution of glycine immunoreactivity in the brain of adult sea lamprey (*Petromyzon marinus*). Comparison with gamma-aminobutyric acid. J Comp Neurol 507:1441–1463.

Villar-Cerviño V, Barreiro-Iglesias A, Fernández-López B, Mazan S, Rodicio MC, Anadón R (2013) Glutamatergic neuronal populations in the brainstem of the sea lamprey, *Petromyzon marinus*: an in situ hybridization and immunocytochemical study. J Comp Neurol 521:522–557.

(Accepted 30 March 2016)
(Available online 4 April 2016)